

# RAMAN LIDAR TECHNIQUES APPLIED TO METEOROLOGICAL SENSING

C. Russell Philbrick  
Penn State University, University Park, Pennsylvania

## ABSTRACT

Raman lidar techniques have been developed and demonstrated which provide measurements of meteorological properties with high spatial and temporal resolution. The vibrational and rotational Raman lidar signals provide simultaneous profiles of water vapor, temperature, ozone and optical extinction due to airborne particulate matter. An operational prototype Raman lidar instrument was prepared and demonstrated for the US Navy and is now used for scientific investigations. It makes use of 2<sup>nd</sup> and 4<sup>th</sup> harmonic generated laser beams of a Nd:YAG laser to provide both daytime and nighttime measurements. The Raman scatter signals from vibrational states of water vapor and nitrogen provide robust profiles of the specific humidity in the lower atmosphere. The temperature profiles are measured using the ratio of rotational Raman signals at 530 and 528 nm from the 532 nm (2<sup>nd</sup> harmonic) beam of the Nd:YAG laser. In addition, the optical extinction profiles are determined from the measured gradients in each of several molecular profiles compared to the molecular scale height. We currently use the wavelengths at 284 nm (nitrogen vibrational Raman), 530 nm (rotational Raman) and 607 nm (nitrogen vibrational Raman) to determine profiles of optical extinction. The ozone profiles in the lower troposphere are measured using a DIAL analysis of the ratio of the vibrational Raman signals for nitrogen (284 nm) and oxygen (278 nm), which are on the steep side of the Hartley band of ozone. Several data sets have been obtained during measurement programs and the results from these events have been the subject of recent investigations. Examples have been selected to show the new level of understanding of meteorological processes that is gained from applications of lidar techniques. These techniques are expected to provide the primary means for profiling meteorological parameters in the future and should provide the data required to constrain the next generation of real time forecasting models.

## 1. INTRODUCTION

Greatly improved meteorological data products are needed by the user community for forecasting, for direct operational support, for validation of next generation satellite sensors and for constraint of the next generation of meteorological models. The data products needed cannot be provided by the surface instruments and balloon sonde techniques currently in use. The most important data products are the profiles of water vapor, temperature and wind velocity. The current use of stations using two or more balloon sondes each day must be replaced because of several factors: 1) cost, 2) extremely limited time resolution data products, and 3) because the disposable battery and instrument package presents an environmental hazard (primarily recognized in antarctica where biodegradable materials last for a long time). Many profiles each hour can be provided by lidar rather than the two releases per day typical of the balloon sondes. The best solution for meeting the data needs of the future is the use of remote sensing instruments, such as lidar and radar techniques.

Important data on a wide range of atmospheric properties will become available from the set of satellite instruments planned for the NPOESS program. However, none of the satellite instruments can provide the data with the required vertical resolution of key parameters in the lower part of the atmosphere. One of the important parameters needed to describe the atmosphere is the height of the planetary boundary layer (PBL), and no instruments are able to provide this from

\*Address: Prof. C.R. Philbrick, Department of Electrical Engineering, Penn State University, University Park, PA 16802  
e-mail crp3@psu.edu

space with useful accuracy. Today, there are about three hundred stations that release two or more sondes each day to provide the primary data on the lower atmosphere. The balloon sonde measurements should be replaced with an automated remote sensing stations which will automatically record, process, and pass the data products to a data servers where it will be available to the many users of meteorological data. The cost of remote sensing stations can be amortized in less than two years, based upon the cost of the disposable instrument package (at two per day) and the personnel salary saved.

Some of the parameters measured with the lidar are not considered to be part of the normal meteorological data set. However, the ozone profiles and the optical extinction are potentially valuable additions to the data set. As we seek to better understand the air quality hazards the information contained in these parameters is very important, even now the metropolitan weather forecasts frequently include ozone and airborne particulate matter qualitative forecasts. The extinction profiles are important for describing visibility conditions for air traffic and are part of the important work on understanding the global climate. Increasing airborne particulate matter (PM) reduces the direct and indirect flux of solar radiation at the surface by initiating more cloud formation, and that changes the planetary albedo. The increase in airborne particulate matter is principally due to combustion products generated by transportation and power generation.<sup>4</sup> Increases in optical scattering caused by airborne particulate matter could result in reduction of global temperature, thus counteracting the increases expected from the greenhouse effect and contribute to a complicated non-linear response.

The goal of upgrading the meteorological data base by providing several profiles each hour will greatly assist

in observing and forecasting for weather systems as they track across the continent. Lidar and radar techniques currently available can measure the key meteorological profiles of temperature, water vapor and wind velocity from the surface through the troposphere. We have demonstrated the Raman lidar capabilities to obtain the water vapor and temperature data from the vibrational and rotational Raman signals.<sup>2,3</sup> The mature development of the meteorological Doppler radar has demonstrated the capability to provide wind profile measurements through the troposphere.<sup>4</sup> We will not describe the radar measurements here but will emphasize the lidar capability.

The most important meteorological parameters measured by the Raman lidar are temperature and water vapor. Temperature is measured from the distribution of the rotational Raman intensity. The specific humidity is measured from the ratio of the vibrational Raman radiation scattered by water vapor and molecular nitrogen. The water vapor is a particularly important tracer of the tropospheric dynamics and is the best marker of the thickness of the planetary boundary layer. Examples from the results of several investigations will be shown as examples of the capability of Raman lidar.

## 2. RAMAN LIDAR DESCRIPTION

Raman scattering is one of the processes that occurs when optical radiation is scattered from the molecules of the atmosphere. It is most useful because the vibrational Raman scattering provides distinct wavelength shifts for species specific vibrational energy states of the molecules and rotational Raman scattering provides a signal with a wavelength shift that depends directly upon the atmospheric temperature.<sup>6</sup> Figure 1(a) shows a diagram of the vibrational and rotational energy levels that are associated with Raman scatter. When a photon scatters from a molecule, the redistribution of the charge cloud results in a virtual energy state. Most of the atmospheric molecules reside in the ground vibrational level because the vibrational excitation corresponds to relatively large energy transitions (tenths of eV), for simple molecules like nitrogen and oxygen, compared to the thermal energy available. Most scattering events result in the return of the molecule to the ground state and the emitted photon has the energy of the initial photon plus/minus the random thermal velocity of the molecule, that is the Doppler broadening. A small fraction of the transitions (order of 0.1%) result in giving part of the photon energy to the molecule, and ending in the first vibrational level (a Stokes transition). The emitted photon energy is decreased by the energy of the vibrational quanta for that molecule. For the small fraction of molecules existing in the vibrational excited level, the unlikely anti-Stokes transition is possible. The relative sensitivity of the scattering from the vibrational and rotational states is indicated by the scattering cross-section values for scattering by a frequency doubled Nd:YAG laser at 532 nm shown in Figure 1(b). The wavelengths of vibrational Raman back scatter signals from the molecules of the water vapor and molecular nitrogen are widely separated from the exciting laser radiation and can be easily isolated

for measurement.<sup>7</sup> The ratio of rotational Raman signals at 528 nm and 530 nm provides a measurement which is sensitive to atmospheric temperature.<sup>8,9</sup> All of the molecules of the lower atmosphere are distributed in the rotational states according to the temperature. By measuring the ratio scattered signals at two wavelengths in this distribution, the temperature can be directly measured. In order to push the lidar measurement capability into the daylight conditions, we have used the "solar blind" region of the spectrum between 260 and 300 nm. The "solar blind" region is darkened by the stratospheric ozone absorption of ultraviolet radiation. Night time measurements are made using the 660nm/607nm ( $H_2O/N_2$ ) signal ratio from the doubled Nd:YAG laser radiation at 532 nm. Daylight measurements are obtained using the 295nm/284nm ( $H_2O/N_2$ ) ratio from the quadruple Nd:YAG laser radiation at 266 nm. A small correction for the tropospheric ozone must be applied. That correction can be obtained from the ratio of the  $O_2/N_2$  signals 278nm/284nm, and from this analysis the ozone profile in the lower troposphere is also obtained.<sup>10</sup> The Raman techniques, which use ratios of the signals for measurements of water vapor and temperature, have the major advantage of removing essentially all of uncertainties, such as any requirement for knowledge of the absolute sensitivity and non-linear factors caused by aerosol and cloud scattering.<sup>11</sup> Optical extinction is measured using the gradient of the measured molecular profile compared with that expected for the density gradient. Since the Raman signal is only scattered from the molecular component of the scattering volume, and difference in the gradient of the signal from that expected due to loss from molecular scattering and absorption can be used to calculate the aerosol extinction.<sup>12-16</sup>

### 2.1. Water Vapor Measurements

The water vapor specific humidity, or mixing ratio, are determined by taking the ratio of the signals from the 1<sup>st</sup> Stokes vibrational Raman shifts for water vapor and nitrogen. The measurement is made with laser transmission at visible (532 nm) and ultraviolet (266 nm) wavelengths. The visible measurement (660/607) is available at night and the ultraviolet measurement (294/284) is available day and night. The ultraviolet measurement is limited to the first 3 km of the atmosphere because of signal loss due to the large scattering cross-section. The ultraviolet water vapor calibration value has remained relatively constant during the past five years, however the visible sensitivity has shown significant changes, possibly due to overload the photomultiplier tube experienced during daylight. Investigation of the stability of the instrument has shown that the variation between the meteorological balloon sonde water vapor and the lidar is about  $\pm 4\%$ , and this is approximately the value expected due to the spatial and temporal differences between the techniques.<sup>16</sup>

## Excited Electronic States

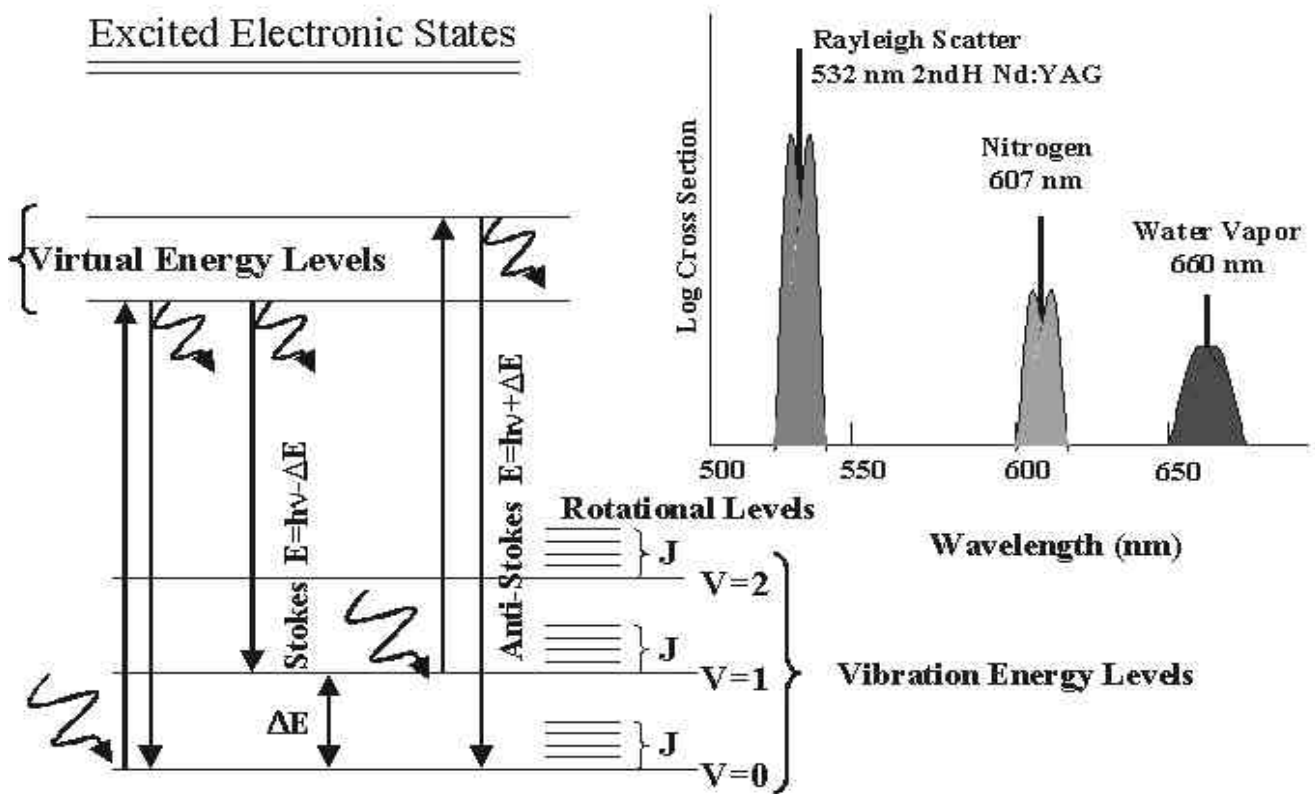


Figure 1. (a) The energy diagram of a molecule illustrates that the scattering of a photon raises the molecule to a virtual level which normally decays to ground ( $V=0$ ) emitting a photon of the same energy as the incident energy, only broadened by thermal Doppler velocity. In a small fraction of cases, the return is Raman shifted to the first vibrational level ( $V=1$ ), a Stokes shift. The relatively large vibrational energy ( $\Delta E$ ) compared with thermal energy makes the Anti-Stokes vibrational transition unlikely, however, the rotational states ( $J$ -levels) are populated by thermal excitation, (b) The relative intensities of the Stokes vibrational Raman shifts of oxygen, nitrogen and water vapor are indicated for illumination of atmospheric molecules with the 532 nm laser. The expected line widths and the relative rotational states are indicated.<sup>6</sup>

Table 2. The LAPS measurements from Raman scatter signals are summarized.

Property	Measurement	Altitude	Time Resolution
Water Vapor	660/607 Raman 294/285 Raman	Surface to 5 km Surface to 3 km	Night - 1 min. Day/Night - 1 min.
Temperature	528/530 Rotational Raman	Surface to 5 km	Night 30 min.
Optical Extinction 530 nm	530 nm Rotational Raman	Surface to 5 km	Night 10 to 30 min.
Optical Extinction 607 nm	607 N <sub>2</sub> - 1 <sup>st</sup> Stokes	Surface to 5 km	Night - 10 to 30 min.
Optical Extinction 285 nm	285 N <sub>2</sub> - 1 <sup>st</sup> Stokes	Surface to 3 km	Day and Night 30 min.
Ozone	276/285 Raman/DIAL	Surface to between 2 and 3 km	Day and Night 30 min.

## 2.2. Temperature Measurements

The rotational states of molecules in the lower atmosphere are populated according to their collision velocity distribution and therefore represents the local temperature. The development of the Raman temperature profiling provides a useful way to measure temperature profiles.<sup>10-12</sup> The rotational state distribution of the nitrogen and oxygen molecules is shown in Figure 2. The temperature is measured using narrow band filters centered near 530 and 528 nm. Since the lower energy states are depopulated and the higher energy states are more populated as the temperature increases.

## 2.3. Ozone Measurements

The Raman vibrational 1<sup>st</sup> Stokes shifts from molecular nitrogen and oxygen are used as the sources for ozone absorption measurement. Since the ratio of these two principal molecular constituents is constant to within 10 ppm in the lower atmosphere, any variation in the vertical profile of this ratio can be associated with the integrated absorption due to ozone. The only other species that has been found to be of concern at these wavelengths is SO<sub>2</sub>, which we have observed in diesel exhaust plumes.<sup>16,17</sup> Figure 3 shows the location of the Raman shifted wavelengths on the sloped side of the Hartley Band. Using the laboratory measured cross-sections in a DIAL lidar inversion analysis, the quantity of ozone can be calculated.<sup>6,12</sup> This technique eliminates the difficult task of tuning and stabilizing the frequency and relative power of the transmitted wavelengths as required for typical DIAL measurements. The fact that the nitrogen and oxygen molecules scatter a known fraction of the two Raman wavelengths in each volume element makes the technique very robust against errors in the measurement.

## 2.4. Optical Extinction Measurements

The extinction coefficient is made up of components due to absorption by chemical species and particles, and scattering by molecules and particles. The Raman scatter signals from the major molecular species provide direct measurements of the optical extinction. The signal at the transmitted wavelength exhibits a profile that combines molecular and particle scattering, and it is difficult to analyze for significant properties, except cloud height. However, analysis of the Raman profiles from molecular scattering signals can provide unique vertical profiles of optical extinction. The LAPS instrument measures the optical extinction profiles from the gradients in each of the measured molecular profiles, at 607, 530 and 284 nm. The wavelength dependent optical extinction can be used to describe changes in the particle size distribution as a function of altitude. These measurements can then be interpreted to determine the air mass parameter and atmospheric optical density. Measurements of optical extinction are based upon gradients in the molecular profiles, using the N<sub>2</sub> vibrational Raman scattering or a band of the rotational Raman lines. The calculation is easily applied to the rotational Raman signal at 530 nm because it is so close to the 532 nm transmitted wavelength that no wavelength dependence exists. By first calculating the extinction at 532 nm from the 530 nm path, it is possible to calculate the optical extinction at 607

nm without assuming a wavelength dependence for aerosol scattering.

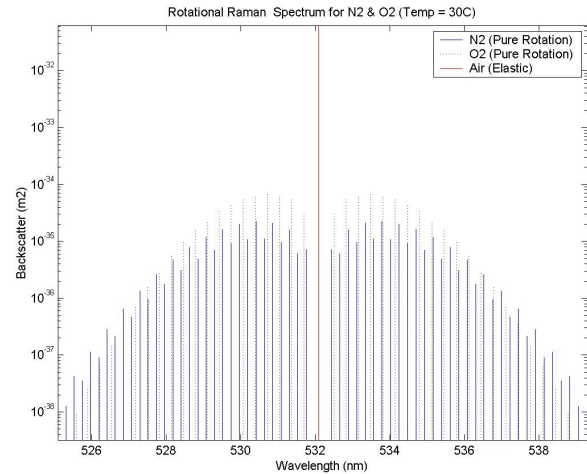


Figure 2. Backscatter cross-sections of the Stokes and anti-Stokes rotational lines of nitrogen and oxygen molecules at 30 C.

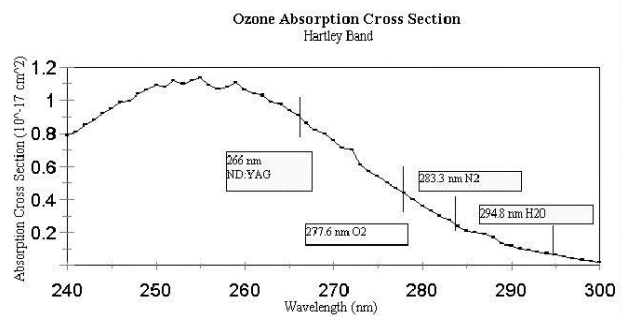


Figure 3. The absorption cross-section of the Hartley band of ozone is shown with the incident and scattered wavelengths indicated.<sup>23</sup>

## 3. EXAMPLES OF RESULTS

The most interesting results from Raman lidar is the multi-dimensional picture of the atmosphere obtained from the time sequence of profiles. Figure 4 shows a time sequence of the temperature data measured on 2 July 1999 during the NARSTO-NE-OPS project in Philadelphia. The time sequence indicates a relatively stable atmosphere during this five hour time period. The small variations in atmospheric temperature are typical. These profiles were calculated each 5 minutes and used a 30 minute smoothing filter.

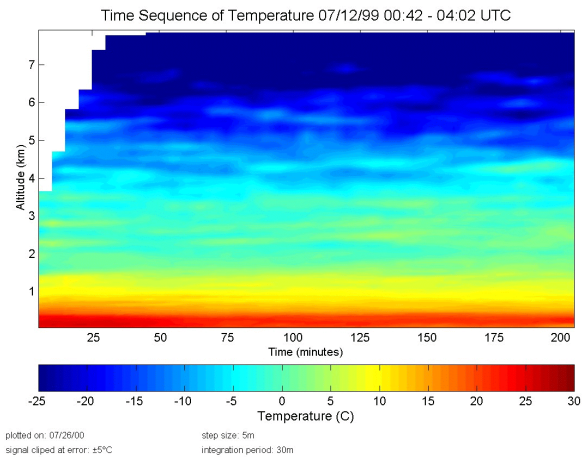
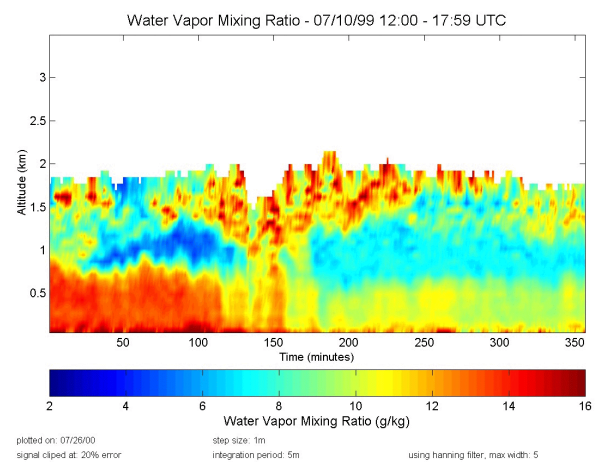
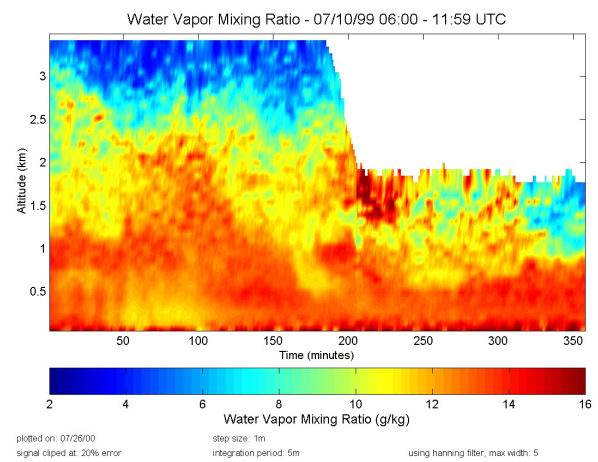
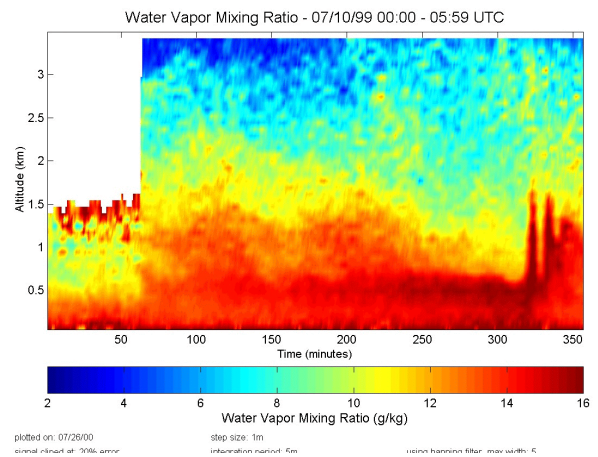


Figure 4. A time sequence of the temperature profiles from the rotational Raman scatter signals shows typical small variations in the air parcels advecting past the vertical lidar beam.

The results in Figure 5 show the variations in water vapor observed during an 18 hour sequence of 1 minute profiles (with a 5 minute smoothing filter) as a front passes through the region on the night of 9-10 July 1999. As the front approached from the northwest, the water vapor increased. During this period of 4-5 hours before the front arrived, the airborne particulate matter and ozone were observed to accumulate ahead of the front. At 0520 UTC (1:20 AM local), the leading edge of the front moved past the site and the large oscillation in the height of the boundary layer occurred. From that time until the trailing edge of the front past the site at 1400 UTC (10 AM local), the area was buffeted by gusty wind and rain. The nighttime data extends to a higher altitude because the scattering and extinction losses in the UV are about 16X those at 532 nm. After the front passes the region (1400 UTC, 1000 local), the air became much dryer as the specific humidity dropped by almost a factor of two. The detail picture provided by a time sequence of the water vapor shows the value of such measurements, particularly if they were available at several locations. Since the LAPS instrument is weatherproof, it was able to operate continuously through the rain periods as the front moved through the region.

The water vapor measurement is obtained from the ratio of the Raman scatter signals from water and molecular nitrogen. The process of using that ratio removes most of the uncertainty and produces a robust measurement. Figure 6 shows a summary of the comparison of the lidar results compared with simultaneous rawinsonde balloons during early tests on the USNS Sumner. A total of 96 rawinsonde balloons were released and all successful balloon flights are compared with the lidar results in these figures. More data points are shown in the ultraviolet plot because comparisons can be made during both day and night. The lidar measures a vertical profile, while the balloon may drift 10's of kilometers away by the time it reaches Figure 5. The time sequences show the water vapor profiles measured as a



front passes through the region.

the tropopause and this can result in significant differences. The  $\pm 4.6\%$  variation in the visible channels approaches the expected differences between the sonde and lidar. The larger 9% variation in the ultraviolet is due to larger statistical error from low photon count signal levels of higher altitude data, and occurs because of the larger ultraviolet extinction.

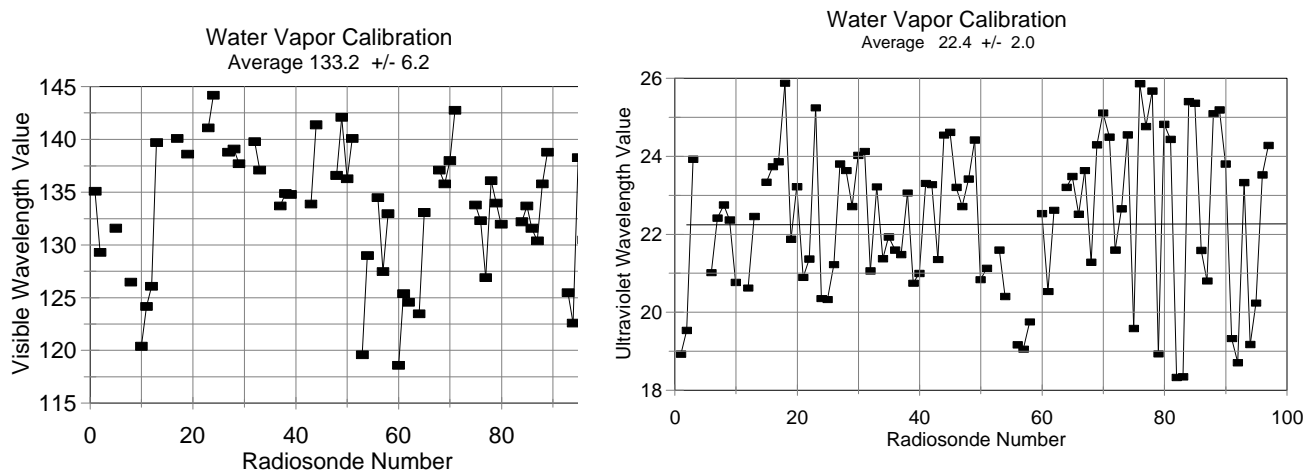


Figure 6. The average ratio of the lidar signal (arbitrary units proportional to specific humidity) to the water vapor measurements from each rawinsonde successfully released from the USNS Sumner.

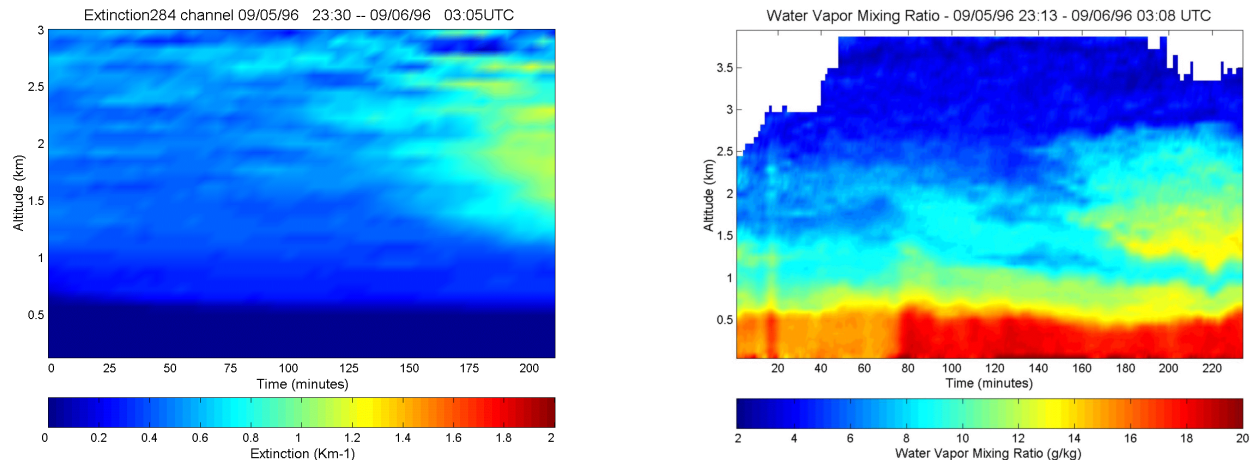


Figure 7. The optical extinction and water vapor measurements on 5 September 1996 on the USNS Sumner show an increase in optical extinction associated with the evolution of a cloud in the same region with enhanced water vapor.

The optical extinction profiles are determined from the gradients in each of the measured molecular profiles, at 607, 530 and 285 nm. The wavelength dependent optical extinction can be used to describe changes in the particle size distribution as a function of altitude for the important small size particles. These measurements can then be used to determine the air mass parameter and atmospheric optical density. Measurements of optical extinction are based upon gradients in the molecular profiles compared to the molecular gradient expected from the temperature profile. Figure 7 shows profiles of aerosol extinction in a time sequence when a cloud developed in the same region. The enhanced water vapor in an aloft layer is associated with the evolutionary development of a cloud. In this case, the cloud is dissipating as it moves into the local area and produces a region of enhanced water vapor at the base of the cloud.

Several interesting examples of results obtained while in the Gulf of Mexico and along the Atlantic coast on the USNS Sumner during the period August thru October 1996 are shown in Figures 7 - 11. Figure 8 shows two examples of the way water vapor is vertically transported and entrained into developing clouds. Each of the white shadow zones indicate where an optically thick cloud has developed. There are several locations in these two examples where the vertical transport of the water into the developing cloud is obvious.

The two examples included in Figure 9 includes a 12 hour sequence of an entire night to show the variations that occur during a relatively stable nocturnal boundary layer. The residual layer is disconnected from the nocturnal boundary layer by the temperature inversion near 500 meters. The residual layer displays its own set of variations and may be changed by transported air.

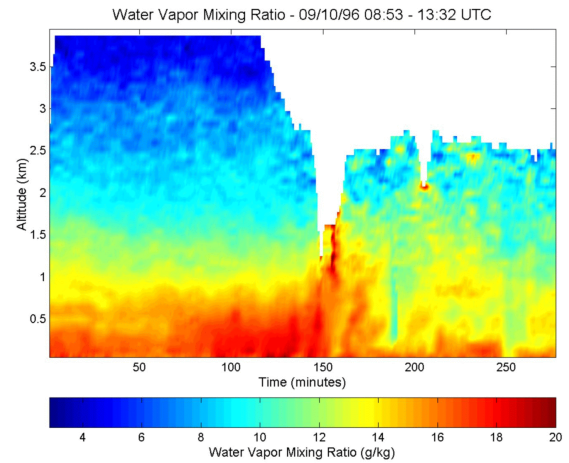
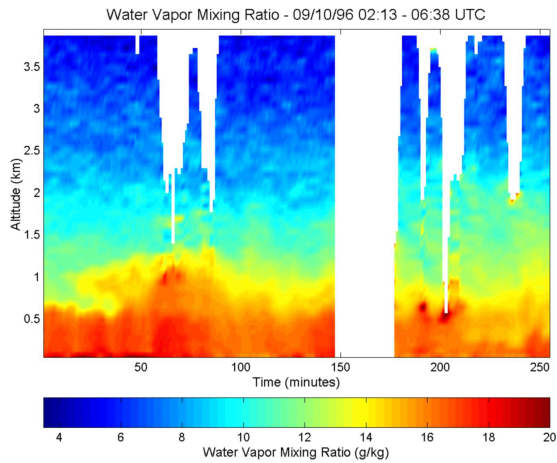
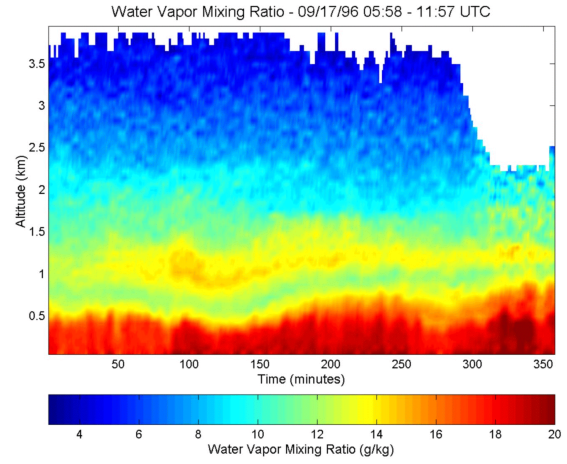
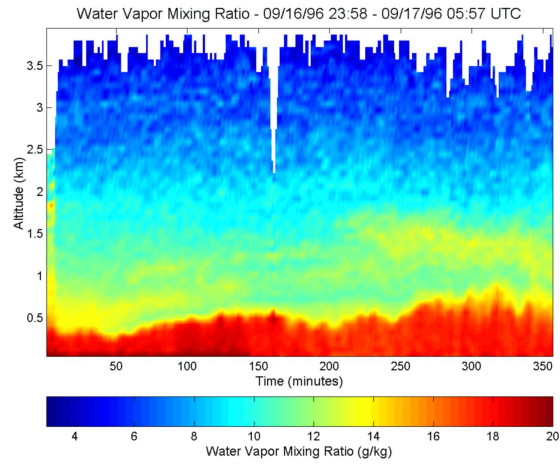


Figure 8. A time sequence on 10 September 1996 using the LAPS instrument onboard the USNS Sumner shows several times when water vapor from the boundary layer is transported up to the base of developing clouds. Figure Figure 9. The time sequences of water vapor profiles show the variations of the nocturnal boundary layer during



a period when the residual layer shows development of a moist layer aloft.

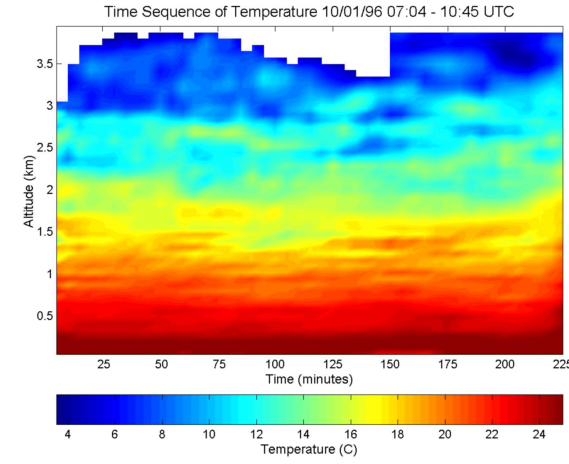
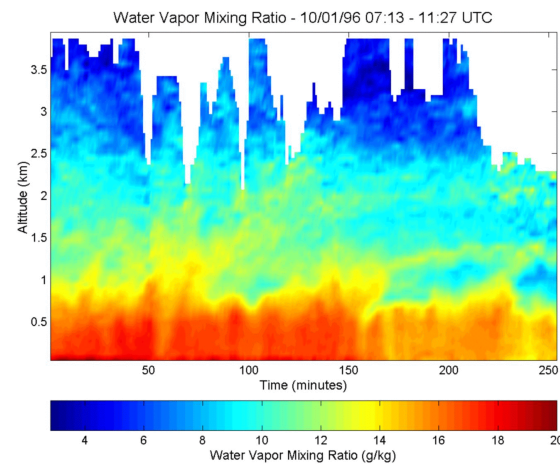


Figure 10. Water vapor and temperature variations shown during an interesting dynamical period.

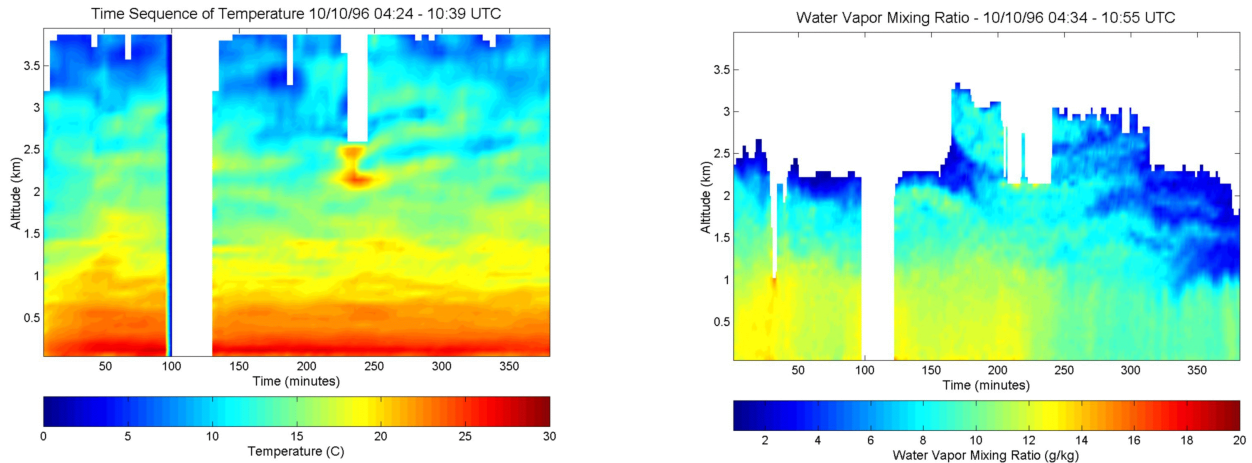


Figure 11. The temperature and the water vapor shown for a dynamically active period during the shipboard testing of the LAPS instrument on the USNS Sumner. At the time 220-240 minutes, a cloud near 2.5 km is observed.

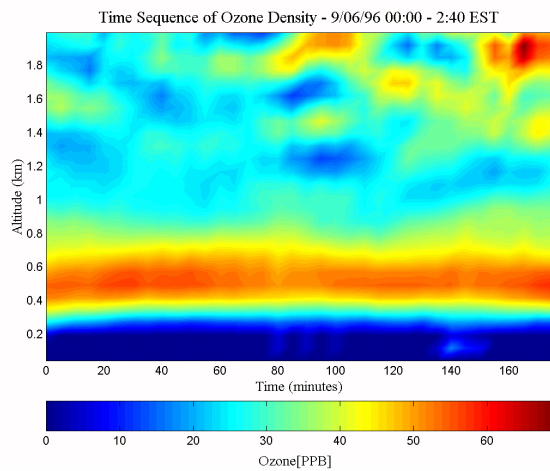


Figure 12. Ozone measurements over the ocean typically show low concentration in the marine boundary layer and moderate concentrations above, these appear to be transported from continental regions.

The results shown in Figure 10 depict the kind of variations that are associated with a very dynamic period. The early morning period is usually a relatively stable period but this example shows an unusual degree of structure in both the water vapor and temperature distribution.

The temperature and water vapor profiles shown in Figure 11 indicate the variations that occur and show the value of having continuous profiles of the important atmospheric properties. When one compares the picture of the development of meteorological conditions from the lidar with that obtained from a few balloon sondes per day, the value of future deployment of lidar instruments becomes obvious.

One of the additional sets of profiles available from

Raman lidar is the ozone, see Figure 12. The results shown here are typical of the shipboard measurements since these are obtained some distance from the production regions for tropospheric ozone. In this case, there is essentially no ozone in the marine boundary layer, below 300 meters. Above the marine boundary layer, ozone appears in a layer which was probably transported from production over the continental land mass.

#### 4. SUMMARY

The goal here has been to provide some examples of the type of meteorological and atmospheric data available from Raman lidar as an indication of what to expect in the future when such instruments replace the balloon sonde as the primary source of data for profiles of meteorological properties.

#### 5. REFERENCES

## REFERENCES

6. Philbrick, C.R., "Raman Lidar Measurements of Atmospheric Properties", *Atmospheric Propagation and Remote Sensing III*, SPIE Vol. 2222, 922-931, 1994.
7. Balsiger, F., and C. R. Philbrick, "Comparison of Lidar Water Vapor Measurements Using Raman Scatter at 266nm and 532 nm," in *Applications of Lidar to Current Atmos. Topics*, SPIE Proc. Vol. 2833, 231-240 1996.
8. Balsiger, F., P. A. T. Haris and C. R. Philbrick, "Lower-tropospheric Temperature Measurements Using a Rotational Raman Lidar," in *Optical Instruments for Weather Forecasting*, SPIE Proc. Vol. 2832, 53-60, 1996.
9. Haris, P.A.T., "Pure Rotational Raman Lidar for Temperature Measurements in the Lower Troposphere," PhD Thesis for Penn State University, Department of Electrical Engineering, August 1995.
10. Esposito, S.T., and C.R. Philbrick, "Raman/DIAL Technique for Ozone Measurements," *Proceeding of Nineteenth International Laser Radar Conference*, NASA/CP-1998-207671/PT1, pp 407-410, 1998.
11. Philbrick, C.R., "Raman Lidar Capability to Measure Tropospheric Properties," *Proceeding of Nineteenth International Laser Radar Conference*, NASA/CP-1998-207671/PT1, pp 289-292, 1998.
12. O'Brien, M.D., T. D. Stevens and C. R. Philbrick, "Optical Extinction from Raman Lidar Measurements," in *Optical Instruments for Weather Forecasting*, SPIE Proceedings Vol. 2832, 45-52, 1996.
13. Philbrick, C.R., M. D. O'Brien, D. B. Lysak, T. D. Stevens and F. Balsiger, "Remote Sensing by Active and Passive Optical Techniques," *NATO/AGARD Proceedings on Remote Sensing*, AGARD-CP-582, 8.1-8.9, 1996.
14. Philbrick, C.R., D.B. Lysak, Jr., M. O'Brien and D.E. Harrison, "Lidar Measurements of Atmospheric Properties," in *Proceedings of the Electromagnetic/Electro-Optics Performance Prediction and Products Symposium*, Naval Post Graduate School, Monterey CA, 385-400, June 1997.
15. Philbrick, C.R., and D.B. Lysak, Jr., "Atmospheric Optical Extinction Measured by Lidar," *Proceedings of the NATO-SET Panel Meeting on E-O Propagation*, NATO RTO-MP-1, pp.40-1 to 40-7, 1998.
16. Philbrick, C.R., and D. B. Lysak, Jr., "Optical Remote Sensing of Atmospheric Properties," *Proceedings of the Battlespace Atmospheric and Cloud Impacts on Military Operations (BACIMO)*, Air Force Research Laboratory, AFRL-VS-HA-TR-98-0103, pg 460-468, 1999.
17. Sedlacek, III, A.J., M.D. Ray and M. Wu, "Augmenting Classical DIAL with Raman-DIAL (RaDIAL)," in *Application of Lidar to Current Atmospheric Topics III*, SPIE Proc. Vol.3757, 126-139, 1999.
18. Measures, Raymond M., *Laser Remote Sensing*. Wiley-Interscience, New York: 1984.
19. Inn, E.C., and Y. Tanaka, "Absorption Coefficient of Ozone in the Ultraviolet and Visible Regions," *J. Optical Society*, **43**, 870-873, 1953.
20. Philbrick, C.R., and D. B. Lysak, Jr., "Lidar Measurements of Meteorological Properties and Profiles of RF Refractivity," *Proceedings of the 1996 Battlespace Atmospheric Conference*, Technical Document 2938 NCCOSC RDT&E, pg 595-609, 1996.
21. Philbrick, C.R., "Investigations of Factors Determining the Occurrence of Ozone and Fine Particles in Northeastern USA," *Proceedings of Symposium on Measurement of Toxic and Related Air Pollutants*, Air & Waste Management Association, pp 248-260, 1998.